JOURNAL OF CATALYSIS **178,** 137–145 (1998)
ARTICLE NO. CA982146

Effect of Promotion with Sn on Supported Pt Catalysts for CO_2 Reforming of CH_4

S. M. Stagg, E. Romeo, C. Padro, and D. E. Resasco[1]

University of Oklahoma, Norman, Oklahoma 73019

Received November 4, 1997; revised April 24, 1998; accepted April 27, 1998

The reforming of CH_4 with CO_2 (dry reforming) was studied at 800°C over SiO_2 and ZrO_2 supported Pt–Sn catalysts. Several preparation methods were investigated. It was found that the Pt/ZrO_2 catalyst had much higher activity and stability than the Pt/SiO_2 catalyst due to the ability of the ZrO_2 to promote CO_2 dissociation. On this catalyst, the decomposition of CH_4 and the dissociation of CO_2 occur via two independent pathways. The long-term activity of the catalyst is dependent upon the balance between the rate of CH_4 decomposition and the rate of cleaning of carbonaceous deposits. The co-impregnation of Sn and Pt on the ZrO_2 results in lower activity and stability than the monometallic catalysts. Depending on the reaction conditions, disruption of the Pt–Sn alloys may occur, causing deposition of tin oxide that inhibits the role of the ZrO_2. Special preparation methods can result in the controlled placement of Sn on the Pt particle, minimizing the promoter–support interaction. These catalysts exhibit higher activity and stability than the monometallic catalyst under severely deactivating conditions, 800°C, and a 3 : 1 ratio of $CH_4 : CO_2$. It is possible to deposit Sn onto Pt/ZrO_2 catalysts in a manner which reduces carbon deposition without inhibiting the beneficial role of the support.

INTRODUCTION

Methane reforming using carbon dioxide (dry reforming) has been of interest for a long time (1–3), but in recent years that interest has experienced a rapid increase both for environmental and commercial reasons (4–12). The major obstacle preventing commercialization of this process is that, due to the endothermic nature of the process, high temperatures are required to reach high conversions. These conditions are conducive to carbon deposition (13), and a catalyst capable of operating at such severely deactivating conditions has not been found. Most of the dry reforming research performed thus far has focused on Group VIII metals on a variety of supports (14–19). Previous work done by our group on SiO_2-supported Pt showed that Sn can be effectively used as a promoter to reduce the amount of carbon deposited during the dehydrogenation of lower alkanes (20). More recently (21) we found that the addition of Sn to a Pt/SiO_2 catalyst decreases carbon deposition and increases the stability of the catalyst during the dry reforming reaction at 650°C.

Several groups have focused on TiO_2 and ZrO_2 and have found that, on these supports, Pt reaches much higher conversions than when supported on SiO_2 and Al_2O_3. Bradford and Vannice have performed an extensive study of Pt/TiO_2 and model TiO_x/Pt catalysts (22, 23). The results from the model catalyst studies indicate that the activity of the catalyst increases with increasing TiO_x coverage. They attribute this increase to the formation of new metal–support interfacial sites and propose that these sites promote the dissociation of CH_4, the dissociation and reduction of CO_2, and the decomposition of CH_xO (23). Also, the formation of TiO_x overlayers on the Pt/TiO_2 catalyst was proposed to increase stability due to suppression of carbon deposition via an ensemble effect (22). Lercher *et al.* (24, 25) have also studied TiO_2 as a support, as well as ZrO_2 and Al_2O_3. They found that, among these three supports, ZrO_2 was the most effective, resulting in a stable catalyst at 600°C and 1 : 1 $CH_4 : CO_2$ feed ratio.

A hypothesis about the role of the support that has received significant attention involves the participation of two independent reaction paths (5, 24, 25). According to this mechanism, CH_4 decomposition would take place on the metal, resulting in the production of H_2 and the formation of carbonaceous deposits. The role of the support would be to adsorb CO_2 and facilitate dissociation at the metal support interface. In this case the CO_2 dissociation would result in CO and adsorbed O. The adsorbed O could then react with carbon deposited on the metal to produce additional CO.

The majority of the previous work on Pt/ZrO_2 catalysts has shown that these catalysts exhibit minimal carbon deposition when operating at relatively moderate temperatures (550–650°C) and the $CH_4 : CO_2$ ratios less than or equal to unity (5, 22, 25). However, the equilibrium conversion of the dry reforming reaction under these conditions is relatively low, i.e., approximately 50%. Furthermore, at low

[1] Corresponding author. E-mail: resasco@ou.edu.

0021-9517/98 $25.00

temperatures and low $CH_4:CO_2$ ratios, a fraction of the H_2 produced is converted to H_2O via the reverse water gas shift reaction, resulting in a H_2/CO product ratio less than one. High conversions and a product ratio near unity can only be achieved near 800°C (15, 26). Most of the concepts developed from the studies conducted at lower temperatures are not valid for the dry reforming reaction at 800°C. It has been shown (27) that hydroxyl groups remain on the surface of the zirconia up to 700°C. These OH groups strongly interact with CO_2, which can generate formate and bicarbonate intermediates. Under industrially relevant conditions, these species may not play a role. Therefore, detailed studies of the reforming reaction at high temperatures are needed. In this contribution, we have investigated ZrO_2-supported catalysts at 800°C, using $CH_4:CO_2$ ratios of 2:1 and 3:1. These high $CH_4:CO_2$ ratios accelerate deactivation by favoring carbon formation. These conditions have allowed us to investigate the role of the support and the promoters in the suppression of carbon formation over relatively short reaction periods.

EXPERIMENTAL

Catalyst Preparation

Pt and Pt–Sn catalysts were supported on SiO_2 (W.R. Grace & Co. Silica Gel Grade 923) and ZrO_2. The ZrO_2 was obtained by calcination of $Zr(OH)_4$ (Magnesium Elektron Inc.) at 800°C for 4 h in stagnant air. A Micromeritics ASAP 2010 adsorption apparatus was used to obtain the physical properties of the supports. After calcination at 800°C, the ZrO_2 support had a BET surface area of 35 m^2/g, and a pore volume of 0.2 cm^3/g. The SiO_2 support, as received, had a surface area of 470 m^2/g, and a pore volume of 0.35 cm^3/g. The monometallic SiO_2- and ZrO_2-supported catalysts had a Pt weight percent of 1.5 and were prepared by incipient wetness impregnation of an aqueous solution of $H_2PtCl_6 \cdot 6H_2O$. The bimetallic sample was made by co-impregnation of $H_2PtCl_6 \cdot 6H_2O$ and $SnCl_2 \cdot 2H_2O$ with 1.5 wt% Pt and a 1:1 molar ratio of Pt:Sn. The incipient wetness liquid/solid ratio was determined for each preparation and varied from 0.3 to 0.5 cm^3/g. The co-impregnated bimetallic catalyst will be referred to as Pt–Sn (CI). Galbraith Laboratories, Inc. performed an elemental analysis on the Pt–Sn (CI) catalyst before and after reaction. The measured percentage of Pt and Sn on the catalyst before reaction was 1.32 and 1.07, respectively. After exposure to a 2:1 ratio of $CH_4:CO_2$ at 800°C for 8 h, the measured percentage of Pt and Sn was 1.40 and 1.11. Two additional ZrO_2-supported bimetallic catalysts were prepared by special techniques. The first involved the co-impregnation of 1.0 wt% Pt and Sn (1:1 molar ratio Pt:Sn) onto a precalcined 1.5 wt% Pt/ZrO_2 catalyst prepared as described above. This catalyst will be referred to as Pt–Sn/Pt. The other preparation method used was surface reduction deposition. Details about this technique, which is intended to selectively deposit Sn on Pt, can be found elsewhere (28). The catalyst was prepared in a solution of *n*-hexane and $Sn(C_4H_9)_4$ at room temperature in He. Prior to the addition of Sn, the 1.0 wt% Pt/ZrO_2 used as a base was reduced *in situ* at 250°C for 1 h and cooled to room temperature in hydrogen. This step results in adsorbed H on Pt, which is responsible for the reduction of the $Sn(C_4H_9)_4$. After the introduction of the Sn solution, the catalyst was washed in clean *n*-hexane and then heated to 60°C in a flow of He. Finally, it was dried for 1 h in He at 150°C. This catalyst (Pt:Sn molar ratio 1:0.5) was reduced *in situ* by heating to 300°C in H_2 (30 cm^3/min) prior to reaction and will be referred to as Pt–Sn (SR). All samples except for the Pt–Sn (SR) were dried overnight at 110°C, calcined in air (30 cm^3/min) at 400°C for 2 h, and then reduced *in situ* for 1 h in H_2 (30 cm^3/min) at 500°C prior to reaction.

Catalyst Activity

The CH_4 reforming activity was measured in a flow reactor consisting of a quartz tube with an inner diameter of 0.4 cm and an outer diameter of 0.6 cm. The experiments on the monometallic and bimetallic catalysts were performed with 0.025 and 0.05 g of catalyst, respectively. Each sample was diluted with an equivalent amount of SiO_2 to minimize heat and mass transfer limitations. A thermocouple was placed directly in contact with the bottom of the catalyst bed during the reaction. A second thermocouple was placed outside the reactor and it was used to control the temperature of the furnace. The Weisz–Prater criteria for internal diffusion was calculated and the results showed that mass transfer limitations were not present in any of the experiments.

The reactions were performed at 650 or 800°C and $CH_4:CO_2$ ratios of 1:1, 2:1, and 3:1. The flow rate was held constant at 75 cm^3/min, resulting in space velocities of 180,000 GHSV and 90,000 GHSV for the monometallic and bimetallic catalysts, respectively. The exit gases were analyzed using an online Hewlett Packard GC equipped with a thermal conductivity detector and a Supelco Carboxen 1006 PLOT fused silica capillary column (30 m, 0.53 mm ID) which allowed for separation of H_2, CO, CH_4, and CO_2. The carrier gas used was Ar. The samples were reduced *in situ*, and then heated to the reaction temperature in Ar (30 cm^3/min). Calibration of the GC using varying ratios of the reactants and products resulted in a mole/area ratio for each gas. Quantification of H_2O was not attempted; however, equilibrium data shows that water production is minimal at high operating temperatures (800°C). The conversion was calculated by dividing the moles of CH_4 and CO_2 converted during reaction by the average of pulses through the by-pass.

Pulse Experiments

Pulse experiments using ^{13}C-labeled CH_4 were performed on the Pt/ZrO_2 and Pt–Sn (CI) catalysts. The samples were heated to 500°C in hydrogen (30 cm^3/min) and reduced for 1 h. After reduction, the samples were heated to 800°C in He (15 cm^3/min) and, while in He, exposed to four pulses of $^{13}CH_4$ (50 μL pulses, 10–15 min apart). During each pulse the exit gases were analyzed using the quadrupole residual gas analyzer. After the $^{13}CH_4$ pulses, the system was flushed for 15 min in He (15 cm^3/min) at 800°C and then exposed to eleven $^{12}CO_2$ pulses. The area of each pulse was converted to moles using a conversion factor that was determined prior to the experiments.

Catalyst Characterization

Extended X-ray absorption fine structure (EXAFS) and X-ray absorption near edge spectroscopy (XANES) were performed on beamline X-18B at the National Synchrotron Light Source at Brookhaven National Laboratory, Upton, New York. The ring energy was 2.5 GeV with a ring current of 80–220 mA. A Si (111) crystal monochromator was used to vary the photon energy incident to the sample. For each sample, 0.5 g of catalyst was diluted with 0.1 g of SiO_2, pressed into pellets and placed into sleeves that were then inserted into a stainless steel cell that can be heated to 650°C or cooled to liquid nitrogen temperatures. The catalysts were reduced *in situ* at 500°C in hydrogen (30 cm^3/min), heated to 650°C in He, and finally exposed to a 2 : 1 ratio of CH_4 : CO_2 at 650°C. After reaction, the samples were cooled to liquid nitrogen temperatures in a flow of He to prevent condensation of water on the samples or oxidation from the atmosphere. EXAFS data were taken near the Pt L_{III} edge (11,564 eV) with the scans ranging from 150 eV below the edge to at least 1000 eV past the edge. The EXAFS data was analyzed using the program BAN from Tolmar Instruments. Details about the analysis procedure can be found elsewhere (29).

RESULTS

Catalytic Activity of the Pt Catalysts

Figure 1 shows the CH_4 and CO_2 conversion for the Pt/ZrO_2 and Pt/SiO_2 catalysts at 650°C. The initial conversions of CH_4 and CO_2 were extremely low on the SiO_2-supported catalyst, and they decreased to almost zero after 30 min on stream. By contrast, the ZrO_2-supported catalyst was much more active and did not deactivate during the 2-h period. The Pt/ZrO_2 sample had a constant H_2 : CO ratio of approximately 0.6 throughout the reaction period, while the ratio for the SiO_2-supported catalyst continuously decreased.

A more drastic deactivation was observed when the same experiment was performed at 800°C. Figure 2 shows the conversion of CH_4 and CO_2 for the Pt/ZrO_2 catalyst during

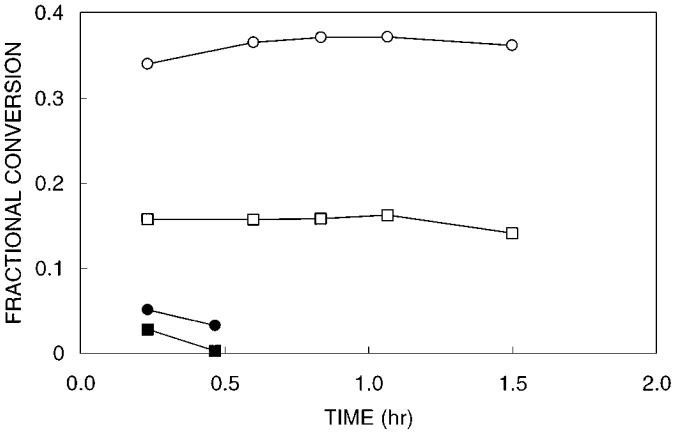

FIG. 1. Fractional conversions of CH_4 (squares) and CO_2 (circles) for Pt/SiO_2 (filled) and Pt/ZrO_2 (open) during reaction at 650°C with a CH_4 : CO_2 ratio of 2 : 1.

20 h of reaction at 800°C with a 2 : 1 CH_4 : CO_2 feed ratio. Initially, the conversion of both CO_2 and CH_4 decreased rapidly, but the decay of the latter was significantly faster. After 4 h on stream, the rate of deactivation decreased with only a slight drop in activity over the next 16 h. The H_2 : CO product ratio was initially 1.0 and decreased to approximately 0.5 by the end of the run. The $X_{(CH_4)}/X_{(CO_2)}$ conversion ratio, which according to the feed composition and stoichiometry of the reforming reaction should be 0.5, was in fact, greater than that at the beginning of the run but decreased to 0.32 with time on stream. Under similar conditions, the Pt/SiO_2 catalysts showed no activity.

Catalytic Activity of the Pt–Sn Catalysts

As shown in Fig. 3, the addition of Sn to the Pt/ZrO_2 catalyst by co-impregnation resulted in a decrease in both the CH_4 and CO_2 conversion when operating at 800°C and

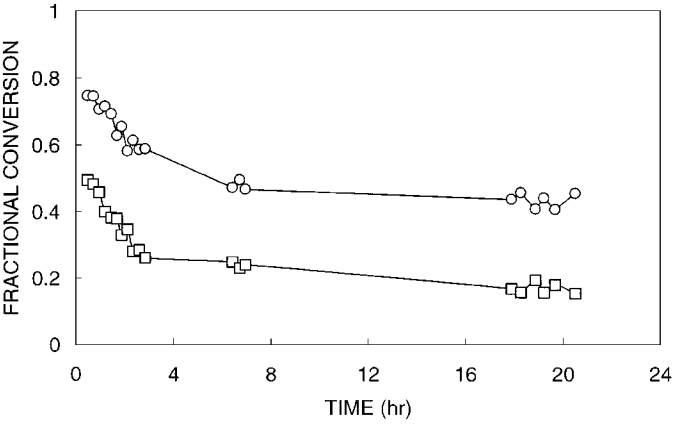

FIG. 2. Fractional conversions of CH_4 (□) and CO_2 (○) for Pt/ZrO_2 during reaction at 800°C with a CH_4 : CO_2 ratio of 2 : 1.

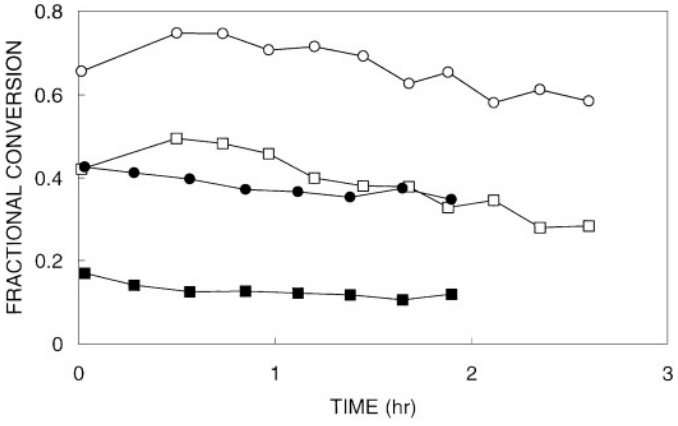

FIG. 3. Fractional conversions of CH_4 (squares) and CO_2 (circles) for Pt–Sn (CI) (filled) and Pt/ZrO_2 (open) during reaction at 800°C with a $CH_4:CO_2$ ratio of 2:1.

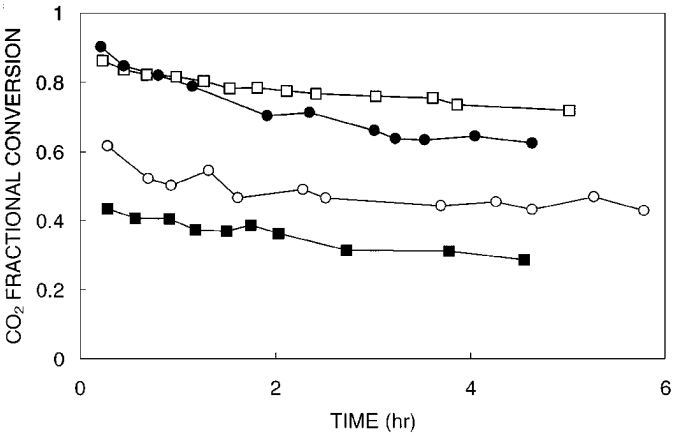

FIG. 5. Fractional conversion of CO_2 for Pt/ZrO_2 (○), Pt–Sn (CI) (■), Pt–Sn/Pt (□), and Pt–Sn (SR) (●) during reaction at 800°C with a $CH_4:CO_2$ ratio of 3:1.

at a feed ratio of 2:1 $CH_4:CO_2$. Although the deactivation rate of the Pt–Sn (CI) catalyst was slightly lower than that of the Pt/ZrO_2 catalyst, the bimetallic sample was less active than the monometallic sample even after 20 h on stream (not shown).

Figure 4 shows the CO_2 conversion for the Pt–Sn/Pt and Pt–Sn (SR) catalysts compared to the Pt–Sn (CI) at 800°C and a 2:1 $CH_4:CO_2$ feed ratio. The conversion of CO_2 was higher for the Pt–Sn/Pt and Pt–Sn (SR) preparations, approaching the conversion of the monometallic sample. Similar trends were observed for the CH_4 conversion. The $H_2:CO$ ratio was measured for both the Pt–Sn (SR) and the Pt–Sn/Pt samples and, during the 20 h of reaction, the values ranged from 0.9 to 0.65 and 0.75 to 0.5, respectively.

When the $CH_4:CO_2$ feed ratio was increased to 3:1, larger differences were observed among the catalysts. Figure 5 compares the CO_2 conversion for all of the ZrO_2-supported samples discussed thus far at 800°C and the higher $CH_4:CO_2$ feed ratio. Under these conditions, the co-impregnated Pt–Sn (CI) exhibited the lowest conversion. On the other hand, the Pt–Sn/Pt and Pt-Sn (SR) catalysts showed much higher activity than both the co-impregnated bimetallic and the monometallic sample. The initial conversion of the Pt–Sn/Pt and Pt–Sn (SR) was 0.88, the same as the Pt catalyst, but the rate of deactivation for the bimetallic samples was much lower, with the conversions after 4 h being 0.75 and 0.68, respectively. Comparison of the two preparations shows that the Pt–Sn/Pt sample exhibited substantially less deactivation than the Pt–Sn (SR) samples. The conversion after 18 h on stream (not shown) was 0.6 for the Pt–Sn/Pt, while the Pt–Sn (SR) had deactivated to approximately 0.3, near the conversion for the monometallic sample.

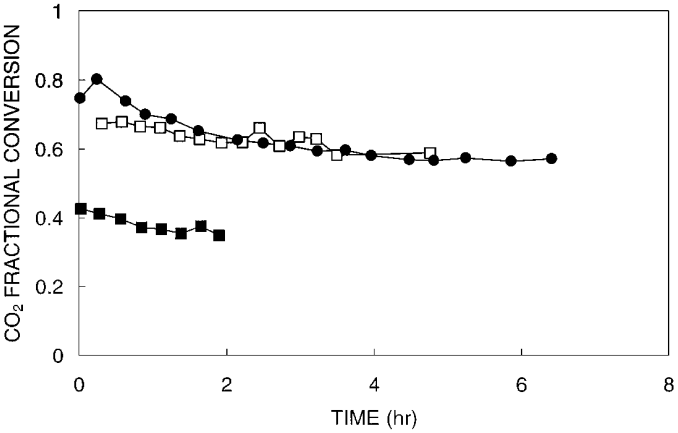

FIG. 4. Fractional conversion of CO_2 for Pt–Sn (CI) (■), Pt–Sn/Pt (□), and Pt–Sn (SR) (●) during reaction at 800°C with a $CH_4:CO_2$ ratio of 2:1.

Figure 6 shows how the activity of a deactivated catalyst was affected by temporarily stopping the flow of one of the reactants for the Pt–Sn/Pt and Pt–Sn (SR) catalysts after reaction at 800°C and a 3:1 ratio of $CH_4:CO_2$. After 18 h of reaction, the flow of CH_4 was stopped and only CO_2 was sent to the reactor. The flow of CH_4 was resumed after 45 min, and the catalyst was again exposed to the reaction mixture. The Pt–Sn (SR) sample showed the greatest increase in CO_2 conversion after stopping the flow of CH_4, reaching approximately 90% of the initial conversion, which as shown in Fig. 5 was about 0.88. However, during the subsequent 2 h of reaction, the activity of the Pt–Sn (SR) catalyst decreased to that of the Pt–Sn/Pt sample. The conversion for the Pt–Sn/Pt catalyst did not increase significantly after exposure to CO_2, but this catalyst experienced a lower extent of deactivation during the initial 18 h on stream. After a subsequent 2-h reaction period, the flow of CO_2 was stopped for 45 min and the catalyst was exposed to CH_4. As shown in Fig. 6, no activity was observed on either catalyst when the flow of CO_2 was resumed.

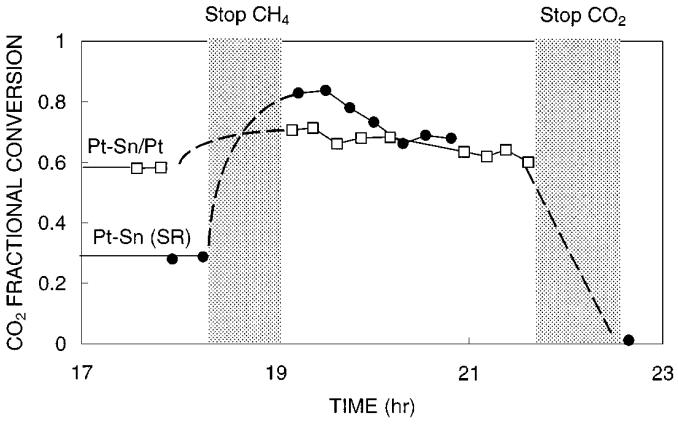

FIG. 6. Effect of temporarily stopping the flow of one of the reactants on the CO_2 conversion for deactivated Pt–Sn/Pt (□) and Pt–Sn (SR) (●) samples after 18 h of reaction at 800°C and 3 : 1 ratio of CH_4 : CO_2.

When similar experiments were performed on the Pt/ZrO_2 and Pt–Sn (CI) catalysts (not shown), they exhibited a very different behavior. The deactivated Pt/ZrO_2 catalyst regained approximately 75% of its initial conversion after stopping the CH_4 flow for 45 min, but it rapidly dropped back to the same conversion. Finally, the deactivated Pt–Sn (CI), unlike the monometallic or the other bimetallic catalysts, did not regain any activity after stopping the CH_4 flow and exposing it to pure CO_2.

$^{13}CH_4$ and $^{12}CO_2$ Pulse Experiments

Figures 7a and 7b show the results of exposing the Pt/ZrO_2 and Pt–Sn (CI) catalysts to pulses of ^{13}C-labeled methane at 800°C. As expected, H_2 was the primary product for both catalysts. However, ^{13}CO and a small amount of $^{13}CO_2$ were also observed. Each subsequent pulse resulted in an increase in the amount of unreacted $^{13}CH_4$ and a decrease in the H_2 and ^{13}CO production.

Following the series of $^{13}CH_4$ pulses, the samples were exposed to 11 pulses of $^{12}CO_2$ (Figs. 8a and 8b). For the Pt/ZrO_2 catalyst, the first two pulses resulted in total conversion of $^{12}CO_2$ into ^{13}CO and ^{12}CO. However, the formation of ^{13}CO and ^{12}CO rapidly dropped after each subsequent pulse, while the amount of unreacted $^{12}CO_2$ increased. On the Pt–Sn (CI) catalyst, the conversion of the $^{12}CO_2$ pulses resulted in almost no ^{13}CO production and a much lower ^{12}CO production than on the Pt/ZrO_2 catalyst.

A similar set of experiments was conducted on the Pt–Sn/Pt (not shown). During the $^{13}CH_4$ pulses, the production of H_2 was less than that observed for both the monometallic and the Pt–Sn (CI) catalysts. However, the amount of ^{13}CO produced was less than that on the monometallic sample, but more than that on the Pt–Sn (CI). Similarly, during the subsequent series of $^{12}CO_2$ pulses the amount of ^{13}CO and ^{12}CO was less than that on the monometallic catalyst, but more than that on the Pt–Sn (CI).

XANES and EXAFS

X-ray absorption studies were performed to determine whether the state of Pt was altered during the reaction due to interaction with the promoter or the support. Before exposure to reaction the XANES spectrum of the Pt/ZrO_2 sample (not shown) looked very similar to that of the Pt foil. The intensity of the first peak (white line) was the same, with only a minor dampening of the second and third oscillations due to the lower coordination of Pt in the catalyst compared to the foil. A slight increase in the intensity of the white line was observed after exposure to reaction at 650°C with a 2 : 1 feed ratio of CH_4 : CO_2. However, the intensity was still much smaller than the white line of an oxidized Pt sample. The effect of Sn on the XANES spectrum for Pt–Sn (CI) catalyst is shown in Fig. 9. Again, the spectra for the sample before and after exposure to the dry reforming reaction are compared to the Pt foil. Unlike the Pt/ZrO_2 catalyst, the intensity of the white line before reaction was

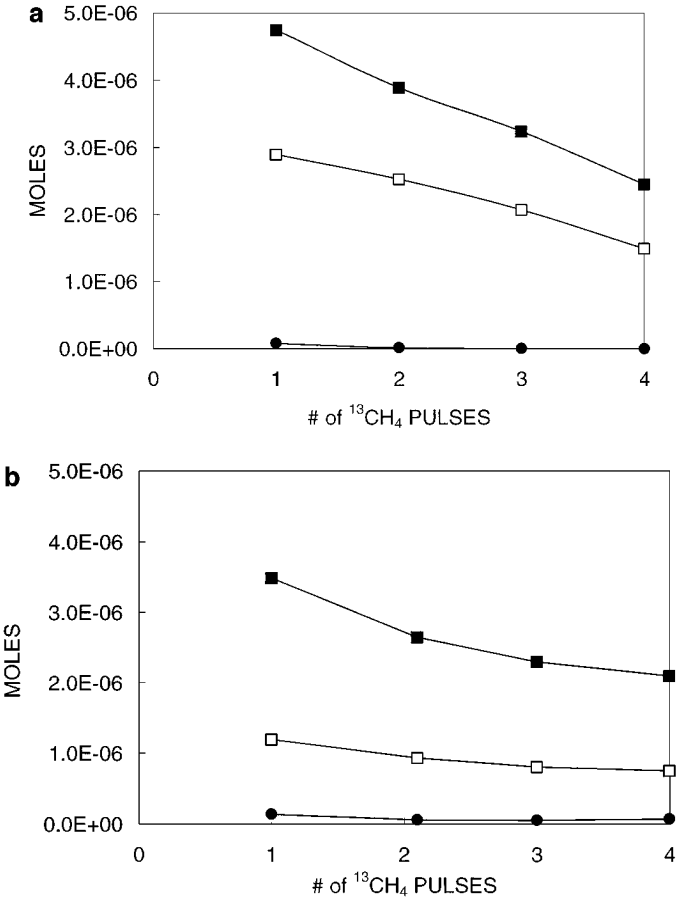

FIG. 7. Moles of H_2 (■), ^{13}CO (□), and $^{13}CO_2$ (●) produced during $^{13}CH_4$ pulses at 800°C over (a) Pt/ZrO_2 and (b) Pt–Sn (CI).

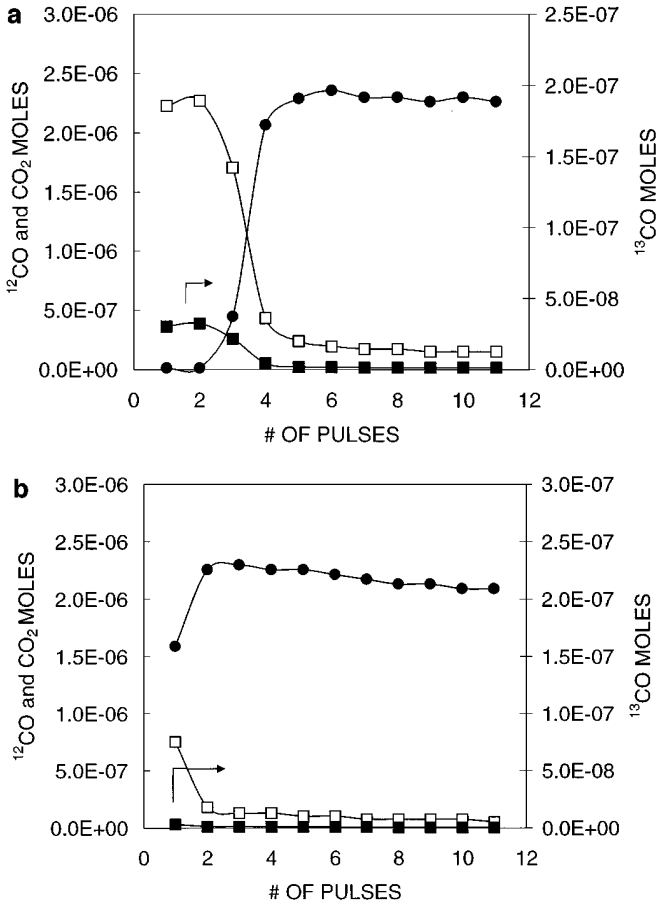

FIG. 8. Moles of ^{13}CO (■), ^{12}CO (□), and $^{12}CO_2$ (●) produced during $^{12}CO_2$ pulses at 800°C after pulses of $^{13}CH_4$ over (a) Pt/ZrO_2 and (b) Pt–Sn (CI).

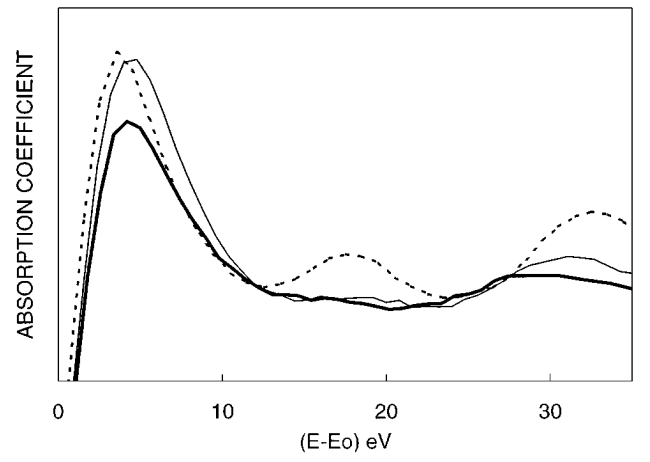

FIG. 9. XANES spectra of Pt foil (---), Pt–Sn (CI) before reaction (——), and Pt–Sn (CI) during reaction at 650°C and a 2 : 1 CH_4 : CO_2 ratio (——).

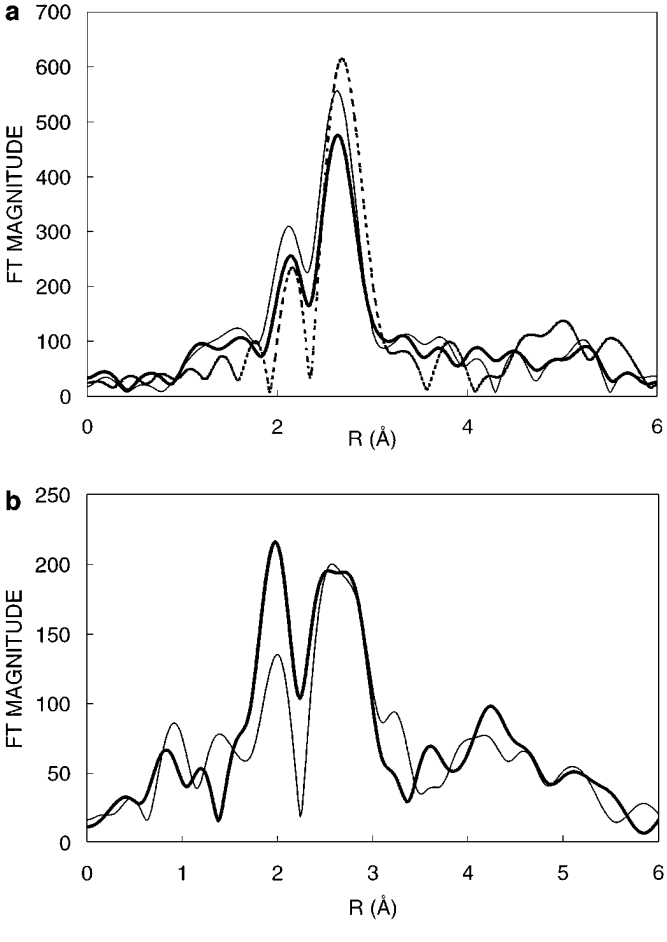

FIG. 10. Fourier transforms of EXAFS data taken at liquid nitrogen temperatures: (a) Pt foil (---), Pt/ZrO_2 before reaction (——), and Pt/ZrO_2 after reaction at 650°C and a 2 : 1 CH_4 : CO_2 ratio (——); (b) Pt–Sn (CI) before reaction (——), and Pt–Sn (CI) after reaction at 650°C and a 2 : 1 CH_4 : CO_2 ratio (——).

much lower than that for the Pt foil. Furthermore, the addition of Sn had a severe dampening effect, which resulted in no significant oscillations beyond the white line. After exposure to reaction conditions, the intensity of the white line of the Pt–Sn (CI) sample was equivalent to that of the Pt foil.

Figure 10a makes a comparison of the EXAFS data for the reduced and spent Pt/ZrO_2 catalysts in comparison to the Pt foil. The main peak corresponds to the Pt–Pt bond distance (2.68 Å before correction, 2.77 Å after correcting for phase and amplitude) with the typical satellite peak at approximately 2–2.1 Å. An increase in the magnitude of the Fourier transform was observed after exposure to reaction. The averaged coordination number under reaction conditions was calculated to be 8.5 ± 0.5. The EXAFS spectra for the bimetallic sample before and after reaction are shown in Fig. 10b. The spectrum of the sample before reaction showed the presence of a peak at approximately 2–2.1 Å, which is much larger than the satellite peak observed at that region for the Pt foil (Fig. 10a). This peak has been observed by other researchers (30) and has recently

been explained as being caused by interference between the Pt–Pt and Pt–Sn bond distances (29). After reaction, a large decrease in the intensity of this peak was observed.

DISCUSSION

The Role of the Support

The results presented in this contribution support the two-path mechanism previously mentioned. During the first 4 h of reaction at 800°C and a $CH_4:CO_2$ feed ratio of 2 : 1 the Pt/ZrO_2 catalyst exhibited a $X_{(CH_4)}/X_{(CO_2)}$ conversion ratio greater than 0.5. The rate of deactivation was also very high for this same period (Fig. 2). This suggests that the rate of CH_4 decomposition is initially greater than the rate of CO_2 dissociation and that the CH_4 decomposition is responsible for the deactivation of the catalyst. As the reaction progressed, both the product ratio and conversion ratio decreased. This is a result of a more pronounced inhibition of the CH_4 decomposition compared to that of the CO_2 dissociation.

In addition, the results of this work show that, in agreement with results from previous authors, the support plays a decisive role. It not only has a strong effect on the activity and stability of the catalyst, but also affects the effectiveness of a promoter such as Sn. When the Pt/ZrO_2 catalyst was exposed to pulses of $^{13}CH_4$, formation of ^{13}CO, together with small amounts of $^{13}CO_2$, was observed (Fig. 7a). Since, the only possible source of oxygen in this experiment was the support, this result suggests that some of the carbon produced from the decomposition of $^{13}CH_4$ was able to partially reduce the oxide support near the perimeter of the particle. The remaining ^{13}C produced from the decomposition of $^{13}CH_4$ was deposited on the Pt metal, possibly as $^{13}CH_x$ species, which explains the observed decrease in the production of H_2 and ^{13}CO with each consecutive pulse. When the same catalyst was subsequently exposed to $^{12}CO_2$ pulses, both ^{12}CO and ^{13}CO were observed. It must be noted that similar experiments performed on ZrO_2 alone showed that, in the absence of Pt, CO_2 dissociation did not occur. These results indicate that Pt is needed to catalyze the dissociation of CO_2. Consequently, either the dissociation takes place near the metal–support interface, or it occurs on oxygen vacancies generated during the previous reduction of the support by the methane pulses. The formation of both ^{12}CO and ^{13}CO supports the idea that carbon is removed from the metal particles under reaction conditions. One possible cleaning mechanism is that the dissociation of CO_2 leads to the formation of CO and adsorbed O which can then combine with carbon on the metal to form additional CO. Another possibility for the cleaning mechanism is that the oxygen that reacts with the carbon comes from the support. In this sense, the support could be acting as a source or sink of oxygen in a redox cycle.

Although the two reaction paths are independent, the stability of the catalyst depends on the balance between the two paths. If the CH_4 decomposition is much faster than the rate of cleaning by CO_2 dissociation, carbon deposition occurs. As shown in the experiments with $^{13}CH_4$ pulses, in the absence of CO_2, the CH_4 decomposition results in the formation of carbon species on the metal, which leads to rapid deactivation. By contrast, if the CH_4 decomposition becomes too slow, the CO_2 dissociation is inhibited. This effect has been observed during the pulses of CO_2 after the $^{13}CH_4$ pulses (Fig. 8a). The dissociation of CO_2 occurred during the first six pulses, while the cleaning stopped after the fourth pulse. It is possible that the O species formed during the dissociation oxidizes the Pt particle near the metal–support interface, preventing further dissociation and cleaning.

Another explanation that has been offered for the differences observed when comparing the activity of various supports is the ability of ZrO_2 to anchor the Pt particles (25). Van Keulen and coworkers (31) have also proposed that ZrO_2 has an anchoring effect, but they explain it in terms of a formation of Pt–Zr surface alloys that help to maintain a high Pt dispersion. Our XANES/EXAFS data do not support the formation of intermetallic compounds; rather they provide evidence that Pt is in an unmodified metallic state.

The low activity observed on the Pt/SiO_2 catalyst could be due to sintering of the Pt particles and subsequent carbon formation on the large Pt agglomerates. It is also possible that the morphology of the support can be greatly altered at high temperatures, causing a large reduction of surface area, which would explain the large activity loss observed. Clearly, on ZrO_2-supported catalysts the support plays a decisive role and they are far superior to other catalysts in which the support does not participate in the reaction.

The Effect of the Addition of Sn

It is well documented that promotion with Sn can result in significant increases in the stability of Pt catalysts (32–34). Catalysts prepared by the co-impregnation of Pt and Sn on SiO_2 had less carbon deposition during dehydrogenation reactions than the unpromoted Pt/SiO_2 catalyst. Studies have shown that, in those cases, the Pt and Sn form a stable alloy and the degree of interaction can vary depending on the preparation method employed (20).

Both the dry reforming and dehydrogenation reactions are highly endothermic, and to achieve high conversions, it is necessary to operate at high temperatures. This is conducive to carbon deposition on the metal particles via the decomposition of the hydrocarbons. It might then be expected that the co-impregnated Pt–Sn catalyst used in the dehydrogenation reaction could result in reduced carbon deposition and increased catalyst stability when employed for the dry reforming reaction.

In fact, previous work (21) has shown that the addition of Sn to Pt/SiO_2 catalysts did reduce the amount of carbon deposited during the dry reforming reaction at 650°C and a 1:1 $CH_4:CO_2$ feed ratio. The bimetallic catalysts were more stable than the monometallic catalysts, and these differences became even more apparent at $CH_4:CO_2$ feed ratios greater than one. The results showed that CH_4 decomposition is responsible for the deactivation of the catalyst due to carbon deposition on the metal. The addition of Sn reduced the formation of carbonaceous deposits by inhibiting the decomposition of CH_4 and resulted in increased stability and a constant product ratio. However, the present contribution shows that, unlike in the case of SiO_2-supported catalysts, the co-impregnation of Sn to the ZrO_2-supported catalyst did not improve the activity or stability of the dry reforming catalyst. Although the addition of Sn hindered the decomposition of CH_4 and decreased carbon formation by this path, the activity of the co-impregnated, bimetallic catalyst was significantly lower than that of the Pt/ZrO_2 catalyst. One explanation for the poor performance of the Pt–Sn (CI) catalyst could be that the presence of Sn disrupts the interaction between the Pt and support at the particle–support interface. It has been previously shown that when Pt–Sn alloys were exposed to an oxidizing atmosphere at high temperatures, the morphology of the catalyst was drastically altered (20, 35). TEM studies (36) have indicated that after oxidation of Pt–Sn catalysts in air, disruption of the alloy occurred, resulting in rings of SnO_2 surrounding a metallic Pt core. It is plausible that the same effects are observed on ZrO_2, especially at temperatures of 800°C, which would completely isolate the Pt particle from the support and eliminate the cleaning mechanism.

X-ray absorption studies performed on the Pt–Sn (CI) catalyst after reaction provide strong evidence for the proposed disruption of the alloy and blocking of the metal-support interface. It is well known (29, 30, 37) that the formation of Pt–Sn alloys results in modifications of the shape of the Pt L_{III} XANES spectra, specifically a decrease in the intensity of the white line. In the case of the zirconia-supported Pt–Sn (CI) catalyst, the XANES spectrum before reaction showed a decreased intensity of the white line, in comparison to that of the Pt reference, indicating the presence of Pt–Sn alloys. However, this intensity increased during the dry reforming reaction. This increase was not due to the oxidation of Pt, because the white line in this case was almost identical to that of the Pt foil reference. Instead, the change can be explained by the disruption of the alloy during the reaction, as proposed above.

At the same time, EXAFS data showed no Pt–O distance, only the two peaks that are related to the Pt–Pt and Pt–Sn bonds. We have recently shown (29) that the simultaneous presence of Pt–Sn alloys and unalloyed Pt gives rise to two peaks in the FT spectrum, one at 2.7 and other at 2–2.1 Å. The intensity of the latter is a good indication of the degree of Pt–Sn interaction. In this case, the short-distance peak greatly decreased under reaction conditions, demonstrating again the disruption of the alloy. The results of the elemental analysis performed on the Pt–Sn (CI) catalyst, before and after reaction, eliminated the possibility that this decrease was due to volatilization and loss of Sn. These results showed that the Sn in the co-impregnated catalyst may become partially oxidized during the dry reforming reaction, leading to disruption of the Pt–Sn alloy.

Further evidence for the disruption of the interaction between the Pt and the ZrO_2 due to the presence of Sn is found in the results of the pulse experiments. In contrast to the Pt/ZrO_2 catalyst, which was very efficient in removing with CO_2 the ^{13}C species deposited during the $^{13}CH_4$ pulses, the Pt–Sn (CI) catalyst only produced a small amount of ^{12}CO and almost no ^{13}CO during the $^{12}CO_2$ pulses. Even though the addition of Sn resulted in decreased carbon deposition, we believe that a negative effect of Sn is to block the interaction of Pt with the support. The effect of this blockage can be observed in both the less efficient reduction of the support during the $^{13}CH_4$ pulses, as well as the decreased carbon removal during the subsequent CO_2 pulses.

In order to minimize the negative effect of Sn we have used preparation methods that allowed for the controlled addition of a small amount of Sn to reduce carbon deposition without disrupting the role of the support. The surface reduction deposition method results in specific placement of the Sn onto the prereduced Pt particle, eliminating the possibility that excess Sn is interacting with the support. This technique also allows for the position of the Sn to be controlled by varying the size of the ligand attached. The intent behind the co-impregnation of Pt and Sn onto the precalcined Pt catalyst was to have the alloy particles on top of Pt particles. In this case, the alloy segregation might be prevented by minimizing the contact between Sn and the support. Figure 4 shows that the Pt–Sn/Pt and Pt–Sn (SR) catalysts have similar activity to the Pt/ZrO_2 catalyst and more than twice the activity of the Pt–Sn (CI) sample. Furthermore, the Pt–Sn/Pt and the Pt–Sn (SR) catalysts were much more stable than the Pt/ZrO_2 and Pt–Sn (CI) at a $CH_4:CO_2$ ratio of 3:1. As mentioned above, the monometallic sample experienced rapid deactivation by carbon deposition due to an imbalance between the rates of decomposition and cleaning. In contrast, the rate of deactivation on the bimetallic catalysts is greatly reduced due to the ability of Sn to inhibit the decomposition of CH_4. However, unlike the Pt–Sn (CI) catalyst, the Pt–Sn/Pt and Pt–Sn (SR) catalysts retain the ability to dissociate CO_2 and facilitate cleaning of the carbon on the metal particle (Fig. 6). This concept is clearly illustrated in the pulse experiments conducted on the Pt–Sn/Pt sample. This work demonstrates that the controlled deposition of Sn can result in a decrease in the

carbon formation by hindering the decomposition of CH_4, without inhibiting the beneficial role of the support.

CONCLUSIONS

In this contribution we have shown that the effect of the addition of Sn on supported Pt catalysts for the dry reforming reaction strongly depends on the reaction conditions, the support, and the preparation methods employed. The main conclusions of this study are as follows:

- The support can play a significant role in the dry reforming reaction by promoting the dissociation of CO_2. This dissociation aids in the removal of carbon deposits from the metal. Supports such as ZrO_2, which facilitate the dissociation of CO_2, exhibit higher activity and stability than those which do not.
- Although the addition of Sn to Pt/SiO_2 improves the stability of the catalyst, the co-impregnation of Pt and Sn on ZrO_2 results in a decrease in the performance. Under reaction conditions, segregation of the Pt–Sn alloy can occur, blocking the interaction between the metal particle and the support.
- In choosing the preparation technique, it is necessary to maximize the Pt–Sn interaction while minimizing the interaction between the promoter and the support. Excess Sn may act to decrease the density of CO_2 adsorption sites near the metal particle, reducing the effectiveness of the support. Preparation techniques such as surface reduction deposition and co-impregnation of Pt and Sn to a precalcined Pt catalyst result in the controlled addition of Sn. These catalysts exhibit higher activity and stability than the monometallic catalyst under severely deactivating conditions, 800°C and a 3 : 1 ratio of $CH_4 : CO_2$.

ACKNOWLEDGMENTS

We gratefully acknowledge the Donors of the Petroleum Research Fund administered by the American Chemical Society and the NSF-CONICET International Program (INT-9415590) for their generous support. We thank the National Science Foundation for a graduate traineeship (SMS). We are grateful to the Ministerio Español de Educacion y Ciencia for a scholarship (ER) and Fundacion Antorchas for travel funds (CP). We also thank the staff of the NSLS at Brookhaven National Labs for their assistance.

REFERENCES

1. Fischer, V. F., and Tropsch, H., *Brennst.-Chem.* **3**(9), 39 (1928).
2. Gadalla, A. M., and Sommer, M. E., *Chem. Eng. Sci.* **44**(12), 2825 (1989).
3. Erdohelyi, A., Cserenyi, J., and Solymosi, F., *J. Catal.* **141**, 287 (1993).
4. Rostrup-Nielsen, J. R., *Stud. Surf. Sci. Catal.* **81**, 25 (1994).
5. Ross, J. R. H., van Keulen, A. N. J., Hegarty, M. E. S., and Seshan, K., *Catal. Today* **30**, 193 (1996).
6. van Keulen, A. N. J., Seshan, K., Hoebink, J. H. B. J., and Ross, J. R. H., *J. Catal.* **166**, 306 (1997).
7. Wang, S. B., and Lu, G. Q., *Energy & Fuels* **10**, 896 (1996).
8. Qin, D., and Lapszewicz, J., *Catal. Today* **21**, 551 (1994).
9. Richardson, J. T., and Paripatyadar, S. A., *Appl. Catal.* **61**, 293 (1990).
10. Zhang, Z. L., and Verykios, X. E., *Appl. Catal. A* **138**, 109 (1996).
11. Solymosi, F., Kustan, G., and Erdohelyi, A., *Catal. Lett.* **11**, 149 (1991).
12. Zhang, Z. L., Tsipouriari, V. A., Efstathiou, A. M., and Verykios, X. E., *J. Catal.* **158**, 51 (1996).
13. Bhat, R. N., and Sachtler, W. M. H., *Appl. Catal. A* **150**, 279 (1997).
14. Rostrup-Nielsen, J. R., and Bak Hansen, J.-H., *J. Catal.* **144**, 38 (1993).
15. Edwards, J. H., and Maitra, A. M., *Fuel Process. Technol.* **42**, 269 (1995).
16. Tsipouriari, V. A., Efstathiou, A. M., Zhang, Z. L., and Verykios, X. E., *Catal. Today* **21**, 579 (1994).
17. Sakai, Y., Saito, H., Sodesawa, T., and Nozaki, F., *React. Kinet. Catal. Lett.* **24**, 253 (1984).
18. Hally, W., Bitter, J. H., Seshan, K., Lercher, J. A., and Ross, J. R. H., *Stud. Surf. Sci. Catal.* **88**, 167 (1994).
19. Kroll, V. C. H., Swaan, H. M., and Mirodatos, C., *J. Catal.* **161**, 409 (1996).
20. Stagg, S. M., Querini, C. A., Alvarez, W. E., and Resasco, D. E., *J. Catal.* **168**, 75 (1997).
21. Stagg, S. M., and Resasco, D. E., *Stud. Surf. Sci. Catal.* **111**, 543 (1997).
22. Bradford, M., and Vannice, M. A., *J. Catal.* **173**, 157 (1998).
23. Bradford, M., and Vannice, M. A., *Catal. Lett.*, in press.
24. Bitter, J. H., Seshan, K., and Lercher, J. A., *J. Catal.* **171**, 279 (1997).
25. Lercher, J. A., Bitter, J. H., Hally, W., Niessen, W., and Seshan, K., *Stud. Surf. Sci. Catal.* **101**, 463 (1996).
26. Krylov, O. V., and Mamedov, A. Kh., *Russ. Chem. Rev.* **64**(9), 877 (1995).
27. Stoppek-Langner, K., Goldwasser, J., Houalla, M., and Hercules, D. M., *Catal. Lett.* **32**, 263 (1995).
28. Margitfalvi, J., Hegedus, M., Gobolos, S., Kern-Talas, E., Szedlacsek, P., Szabo, S., and Nagy, F., *in* "Proceedings, 8th Inter. Congr. Catal., Berlin, 1984," Vol. IV, p. 903. Dechema, Frankfurt-am-Main, 1984.
29. Borgna, A., Stagg, S. M., and Resasco, D. E., *J. Phys. Chem.* (in press).
30. Meitzner, G., Via, G. H., Lytle, F. W., Fung, S. C., and Sinfelt, J. H., *J. Phys. Chem.* **92**, 2925 (1988).
31. van Keulen, A. N. J., Hegarty, M. E. S., Ross, J. R. H., and van den Oosterkamp, P. F., *in* "Natural Gas Conversion Meeting, South Africa, Nov. 1995."
32. Yarusov, I. B., Zatolokina, E. V., Shitova, N. V., Belyi, A. S., and Ostrovskii, N. M., *Catal. Today* **13**, 655 (1992).
33. Barias, O. A., Holmen, A., and Blekkan, E. A., *Catal. Today* **24**, 361 (1995).
34. Cortright, R. D., and Dumesic, J. A., *Appl. Catal. A* **129**, 101 (1995).
35. Verbeek, H., and Sachtler, W. M. H., *J. Catal.* **42**, 257 (1976).
36. Chojnacki, T. P., and Schmidt, L. D., *J. Catal.* **129**, 473 (1991).
37. Ross, P. N., *J. Vacuum Sci. Technol.* **10**, 2546 (1992).